

# Membrane Topology of the STT3 Subunit of the Oligosaccharyl Transferase Complex\*<sup>§</sup>

Received for publication, October 28, 2004, and in revised form, February 16, 2005  
Published, JBC Papers in Press, March 21, 2005, DOI 10.1074/jbc.M412213200

Hyun Kim, Gunnar von Heijne, and IngMarie Nilsson<sup>‡</sup>

From the Department of Biochemistry and Biophysics, Stockholm University, SE-10691 Stockholm, Sweden

**The highly conserved membrane protein STT3 is part of the oligosaccharyl transferase complex in the endoplasmic reticulum of eukaryotic cells. Various experimental observations strongly suggest that STT3 contains the active site of the complex. Here, we report a detailed topology study of STT3 from two different organisms, *Saccharomyces cerevisiae* and mouse, using *in vivo* and *in vitro* topology mapping assays. Our results suggest that STT3 has 11 transmembrane helices and an overall  $N_{\text{cyt}}\text{-}C_{\text{lum}}$  orientation.**

STT3 is a highly conserved polytopic membrane protein found in all eukaryotic organisms. It was first discovered as a staurosporine- and temperature-sensitive mutant in *Saccharomyces cerevisiae* (1) and was later found to be a subunit of the hetero-oligomeric oligosaccharyl transferase (OT)<sup>1</sup> complex (2). Systematic site-directed mutagenesis in combination with photo-cross-linking using a derivatized peptide carrying an *N*-linked glycosylation consensus sequence suggested a direct involvement of Stt3p in substrate recognition (3).

Mammalian cells express two homologues of Stt3p (STT3-A and STT3-B) that form a complex with other OT subunits (ribophorins I and II, OST48, and DAD1) (4). STT3-A and -B are expressed in a tissue-specific manner and modulate the enzymatic activity of OT (4). A photoreactive probe incorporated into a nascent polypeptide chain carrying a cryptic glycosylation sequon (Gln-X-Thr) can be cross-linked to STT3-A in dog pancreatic microsomes (5), lending further support to the idea that STT3 is the catalytic subunit of OT. An STT3 homologue has recently been discovered in the enteropathogenic bacterium *Campylobacter jejuni* (6), in which *N*-linked glycosylation of secretory proteins also occurs on the consensus sequence Asn-X-Thr/Ser.

STT3 is the most conserved of the known OT subunits (7). Stt3p from *S. cerevisiae* has 50% sequence identity to the human homologues, and highly conserved stretches of residues are found throughout the protein. In particular, absolute conservation is observed in some of the loops between the pre-

dicted transmembrane helices (TMs) in the N-terminal half of the protein and in the region around the proposed active site in the C-terminal domain (7).

Despite its central role in *N*-linked glycosylation, little information on the membrane topology of STT3 is available. A C-terminal protein A fusion to *S. cerevisiae* Stt3p has located the C terminus of the protein to the luminal side of the endoplasmic reticulum (ER) membrane (2), but the number of transmembrane helices and their orientations relative to the membrane have not been determined.

Here, we present *in vivo* and *in vitro* topology mapping studies of *S. cerevisiae* Stt3p and mouse STT3-A, using C-terminal reporter fusions and insertion of glycosylation sites in the loops between the putative transmembrane segments. We propose a common  $N_{\text{cyt}}\text{-}C_{\text{lum}}$  topology with 11 transmembrane helices for the STT3 family of proteins.

## EXPERIMENTAL PROCEDURES

**Yeast Plasmid Construction and Transformation**—For construction of plasmids with a Suc2 segment insertion, a SphI site was generated by the Stratagene QuikChange site-directed mutagenesis kit (Stratagene, La Jolla, CA) in the desired position in the *STT3* gene in plasmid pRS314STT3HA (3). Homologous recombination regions were chosen as the upstream and downstream 33 bp flanking the SphI site. A segment of the *SUC2* gene encoding residues 81–133 was amplified by PCR from plasmid pJK90 (8) using a forward primer composed of the homologous region chosen upstream of the SphI site in pRS314STT3HA and 17 bases complementary to the 5' end of the *SUC2* segment and a reverse primer composed of 17 bases complementary to the 3' end of the *SUC2* segment and the 33-bp recombination region downstream of the SphI site in pRS314STT3HA. Yeast transformation was carried out in strain STY50 (MAT a, *his4-401*, *leu2-3*, *112*, *trp1-1*, *ura3-52*, *HOL1-1*, *SUC2::LEU2*) (9) with a SphI-digested pRS314STT3HA-(N (N-terminal), 105, 113, 139, 354, 385, 404, 440, C (C-terminal)) and the *SUC2* PCR product. Colony PCR was carried out on each transformant using a 5' primer complementary to the upstream sequence of the *STT3* gene in pRS314STT3HA (5'-ACTTCTCTTCGCCTCTGC-3') and a 3' primer complementary to a region within the *SUC2* insert (5'-TTGCTTGATCAATAG-3'). Positive colonies were selected, and plasmid was isolated and transformed into *Escherichia coli* for sequencing. After confirming the correct sequence of the construct, plasmid was transformed into strain QYY700 (MAT a *ade2 can1 his3 leu2 trp1 ura3 Δ stt3::his5+* (*Schizosaccharomyces pombe*) YEp352-*STT3*) (3), and transformants were selected on  $-Ura/-Trp$  plates. Plasmids encoding truncated Stt3p fused to a C-terminal HA/Suc2/His4C reporter were constructed as described (10) and transformed into strain STY50 (9).

Plasmids carrying truncated Stt3p with a Suc2 insertion were constructed as follows. First, pJK90 was digested with XhoI, linearizing the plasmid in between HA and the start of the *SUC2* gene. In addition, for homologous recombination, the XhoI-digested pJK90 was transformed with STY50 strain and the PCR-amplified *HIS8* with a stop codon (two primers, 5'-GGCTCTATCCATATGACGTTCCAGATTACGCTGCGGCCATCATCATC-3' and 5'-ATCGCTAGTTTCGTTTGTCTATCCCCCGGATCTCAGTGGTGGTGGTGG-3', were used). Positive clones carrying HA/*HIS8* tag were selected by colony PCR, and the correct sequence was confirmed by DNA sequencing and named pJK95. Second, to amplify truncated Stt3p with a Suc2 insertion, PCR was carried out with two primers (5'-GTTTGTACGCATGCAAGCTTGATATCGAAATGGGATCCGACCGTCTG-3' and 5'-GTGGTTTGC-

\* This work was supported by grants from the Swedish Cancer Foundation (to I. N. and G. v. H.), from the Swedish Research Council (to G. v. H.), from the Swedish Foundation for International Cooperation in Research and Higher Education (to I. N.), and from Magnus Bergvalls Stiftelse (to I. N.). The costs of publication of this article were defrayed in part by the payment of page charges. This article must therefore be hereby marked "advertisement" in accordance with 18 U.S.C. Section 1734 solely to indicate this fact.

<sup>§</sup> The on-line version of this article (available at <http://www.jbc.org>) contains select STT3 hits from PBLAST via Expasy.

<sup>‡</sup> To whom correspondence should be addressed. Tel.: 46-8-162728; Fax: 46-8-153679; E-mail: [ingmarie@dbb.su.se](mailto:ingmarie@dbb.su.se).

<sup>1</sup> The abbreviations used are: OT, oligosaccharyltransferase; ER, endoplasmic reticulum; 5FOA, 5-fluoroorotic acid; TM, transmembrane; Endo H, endoglycosidase H; TMHMM, transmembrane hidden Markov model.

TTACGCATGCAAGCTTGATATCGAAATGGGATCCGACCGTGCG-3') and pRS314STT3HA with Suc2 insertions at various positions as a template. PCR products and an SmaI-digested pJK95 were transformed into STY50, and positive clones were selected on -Ura plates.

**Membrane Fractionation and Endo H Digestion**—Membrane fractions were prepared as described in Ref. 11 with some modifications. Yeast transformants were grown overnight in 5 ml of auxotrophic media. Cells were harvested and washed with 5 ml of distilled H<sub>2</sub>O and resuspended in 200  $\mu$ l of cold lysis buffer (20 mM Tri-HCl, pH 7.6, 10 mM EDTA, 0.1 M NaCl, 0.3 M sorbitol, 1 mM phenylmethylsulfonyl fluoride, 1 mM benzamidine, Complete protease inhibitor mixture from Roche Applied Science) and transferred to a 2-ml Eppendorf tube containing 200  $\mu$ l of acid-washed glass beads (Sigma). Cell suspensions were vortexed 5 times at full speed for 45 s with 30-s intervals on ice. Cell suspension excluding glass beads was transferred to a new tube on ice, the glass beads were washed once with 200  $\mu$ l of lysis buffer, and this residual cell suspension was added to the first tube. The glass bead-treated cell suspension was centrifuged for 5 s to remove unbroken cells, and the soluble fraction was transferred to a new tube and centrifuged at 14,000 rpm for 30 min at 4 °C. The membrane pellet was resuspended with 100  $\mu$ l of Endo H buffer (80 mM sodium acetate, pH 5.6, 1% SDS, 1%  $\beta$ -mercaptoethanol) and centrifuged at 14,000 rpm for 5 min, and the pellet was discarded. 30  $\mu$ l of each soluble fraction was aliquoted into two tubes; 1  $\mu$ l of Endo H (5 units/ml) was added to one tube, and the other tube was used as a mock sample.

**Western Blotting Analysis**—All Endo H-digested samples were analyzed by 10% SDS-PAGE followed by Western blotting. The blot was probed with anti-HA mouse antibody (Covance Research Products, Richmond, CA) and developed using the ECL Advance Western blotting detection kit (Amersham Biosciences).

**Growth Assay**—Yeast transformants carrying pJK92-derived Suc2/His4C reporter fusion plasmids were streaked on -His plates supplemented with 6 mM histidinol and incubated at 30 °C for 3 days. Yeast transformants carrying *SUC2* insertion plasmids were streaked on 5FOA plates and incubated at 30 °C for 2 days.

**Plasmid Construction and in Vitro Expression of Mouse STT3-A**—Mouse STT3-A constructs were made as described previously (12). Briefly, for cloning into and *in vitro* expression from the pGEM1 plasmid, the 5' end of the *Itm1* gene encoding STT3-A (GenBank™ accession number L34260) in the pSPORT1 plasmid (13) was modified in two ways during PCR amplification: (i) by the introduction of a 5' XbaI site and (ii) by changing the context of the region immediately upstream of the initiator ATG codon to a Kozak consensus ribosome binding sequence, CCACCATGG (12, 14); both changes were encoded within the 5' PCR primer. The reverse primer encoded the 3' end of *STT3*, two stop codons, and an SmaI site for cloning. The *STT3* gene was amplified by PCR using the Expand Long Template PCR system from Roche Diagnostics and cloned into pGEM1 downstream of the SP6 promoter as an XbaI-SmaI fragment.

Templates for *in vitro* transcription of truncated mRNA with a 3' stop codon were prepared using PCR to amplify fragments from the pGEM1 plasmids containing the relevant *STT3* constructs. The 5' primers were the same for all clones and were situated 210 bases upstream of the translational start such that all amplified fragments contained the SP6 promoter from pGEM1 (15). The 3' primers were designed according to the desired C-terminal end of the truncated protein, and tandem stop codons (TAA TAG) were introduced after codons 198, 280, 310, 498, 538, and 543 in the *Itm1* gene. The amplified DNA products were purified using the QIAquick PCR purification kit from Qiagen (Hilden, Germany).

Glycosylation acceptor sites were designed as described previously (16), *i.e.* by replacing one, two, or three appropriately positioned codons with codons for the acceptor tripeptide Asn-Ser-Thr, by insertion of one or more codons for the acceptor tripeptide Asn-Ser-Thr, or by combining these two methods. In one case, a loop in the STT3-A protein was elongated by 10 residues using spacer sequences flanking an acceptor Asn-Ser-Thr tripeptide.

Site-specific mutagenesis was performed using the QuikChange™ site-directed mutagenesis kit from Stratagene. All mutants were confirmed by sequencing of plasmid DNA at BM labbet AB (Furulund, Sweden). All cloning steps were done according to standard procedures using restriction enzymes from Promega (Madison, OH).

The DNA template for *in vitro* transcription was prepared by transcription of the relevant pGEM1-derived plasmid with SP6 RNA polymerase for 1 h at 37 °C. mRNA translation in nuclease-treated reticulocyte lysate supplemented with [<sup>35</sup>S]Met was performed as described (17) at 30 °C for 1 h. All Endo H-digested samples were performed as described above. Samples were analyzed by SDS-PAGE, and proteins

were visualized in a Fuji FLA-3000 phosphorimaging device using the Image Reader V1.8J/Image Gauge V 3.45 software.

## RESULTS

The membrane topology models for yeast Stt3p and mouse STT3-A predicted by the TMHMM method (18) are shown in Fig. 1. The predicted topologies differ in the number of transmembrane segments (13 for yeast, 12 for mouse) and in the location of the hydrophilic C-terminal domain (luminal in yeast, cytosolic in mouse). Guided by these predictions, we engineered glycosylation sites in most of the predicted loops and also made in-frame and C-terminal truncation reporter fusions to obtain further data on the topology of the two proteins.

***S. cerevisiae Stt3p***—We have taken two approaches to investigate the membrane topology of yeast Stt3p. The first is to insert a 52-residue-long segment of invertase with three *N*-glycosylation sites into predicted loops of full-length Stt3p, and the second is to fuse the dual Suc2/His4C topology reporter (10, 19) at the C terminus of truncated Stt3p molecules. In the first approach, glycosylation of the invertase fragment indicates a luminal location of the corresponding loop; in the second approach, glycosylation of the reporter again suggests a luminal orientation, whereas the ability of transformed *his4<sup>-</sup>* cells to grow on media lacking histidine but including histidinol suggests a cytosolic location of the reporter (19). In both approaches, a hemagglutinin tag was attached to Stt3p to allow detection by Western blotting.

To insert the invertase fragment into Stt3p, we amplified an internal part of the *SUC2* gene encoding a 52 amino-acid segment (residues 81–133) that contains three *N*-glycosylation sites. It has been shown previously that insertion of this fragment into other *S. cerevisiae* membrane proteins does not influence the overall topology (20). The invertase fragment was inserted into predicted loops as detailed in Table I.

The constructs were transformed into an *stt3* deletion strain carrying the wild-type *STT3* gene on a plasmid with a URA marker (3). Since *STT3* is an essential gene in *S. cerevisiae*, wild-type *STT3* must be present on a plasmid for a haploid deletion strain to survive. To test whether the different constructs can functionally replace Stt3p, transformants were streaked onto 5FOA plates. If the Stt3 insertion construct can replace wild-type *STT3*, transformants will grow on 5FOA plates by releasing the URA3 plasmid carrying wild-type *STT3*. In contrast, if the construct does not complement the loss of wild-type Stt3p, cells cannot be cured of the wild-type *STT3* plasmid and thus die on 5FOA plates due to the accumulation of toxic fluorodeoxyuridine that is formed from 5FOA and uracil in the cell.

Of the different insertion constructs, the ones with insertions at residues 105 and 204 showed a very low level of protein expression (data not shown). The constructs with insertions after residues 354 and 404 expressed detectable levels of protein, but the transformants did not grow on 5FOA (data not shown). The remaining transformants allowed growth on 5FOA (Fig. 2A), showing that these insertions are compatible with Stt3p function and thus presumably allow a significant fraction of the molecules to insert with the correct topology.

To determine the location (cytosolic or luminal) of the invertase fragment in these constructs, membrane fractions were prepared from yeast transformants expressing the different constructs and subjected to Endo H digestion. Wild-type Stt3p migrates anomalously as a smeared band with an apparent molecular mass of ~60 kDa (21). As expected, the constructs with a Suc2 insertion migrated more slowly than wild-type Stt3p (Fig. 2B). The WT (wild type), N (N-terminal), 139, 385, and 440 Suc2 insertion showed only a minor mobility shift upon

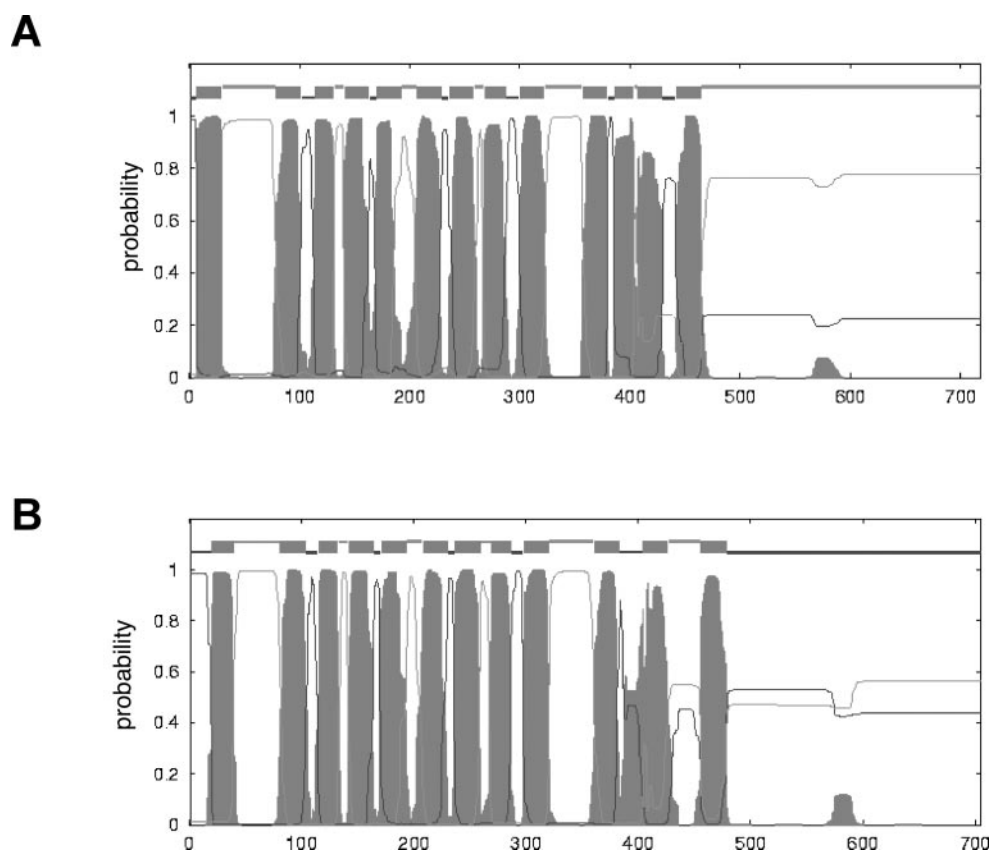


**FIG. 1. Topology predictions for yeast (A) and mouse (B) STT3 using the TMHMM prediction method.** Yeast Stt3p is predicted to have 13 TMs and the C-terminal domain in the lumen, whereas mouse STT3-A is predicted to have 12 TMs and the C-terminal domain in the cytoplasm. Transmembrane segments (gray rectangles), cytoplasmic loops (thin black line), and luminal loops (thin gray line) are indicated above the curves that show the *a posteriori* probabilities for the different locations.

TABLE I  
Summary of the results

In column 1, (y) indicates yeast Stt3p, and (m) indicates mouse STT3-A. In column 2, *I* indicates insertion of the Suc2 glycosylation domain in full-length yeast Stt3p, *I-t* indicates insertion of the Suc2 in truncated yeast Stt3p, *N* indicates *in vitro* translation of mouse STT3-A with an added glycosylation site, and *T* indicates a Stt3p fusion to the Suc2/His4C reporter domain.

Position of the residue	Modification	Complementation of <i>stt3</i> deletion	Orientation
N(y)	I	Yes	Cytosol
2(m)	N		Cytosol
56(m)	N		Lumen
74(m)	N		Lumen
78(m/y)	N/T		Lumen
105(y)	I-t		Lumen
113(y)	I(I-t)	Yes/weak	Lumen
139(y)	I(I-t)	Yes/weak	Cytosol
140(y)	T		Lumen
185(m)	N		See Results
199(y)	T		Lumen
235(y)	T		Cytosol
296(y)	T		Cytosol
340(m/y)	N/T		Lumen
354(y)	I(I-t)		Lumen
385(y)	I(I-t)	Yes	Cytosol
386(y)	T		Lumen
437(y)	T		Cytosol
440(y)	I(I-t)	Yes	Cytosol
441(m)	N		Cytosol
515(m)	N		Lumen
C(m/y)	N/I	Yes	Lumen

Endo H treatment (Fig. 2B), reflecting the only endogenous glycosylation site at Asn<sup>535</sup> in the C-terminal domain (22). Thus, the Suc2 reporter domain in these constructs is not glycosylated, suggesting that the loops where the Suc2 domain

was inserted are oriented to the cytosolic side of the ER membrane.

In contrast, insertion of the Suc2 domain after amino acid residue 354 and at the C terminus resulted in a larger molecular weight difference between Endo H non-treated and treated samples (Fig. 2B), suggesting that the reporter domain was glycosylated and thus located in the lumen of the ER. Endo H treatment of the construct with an insertion after amino acid residue 113 resulted in a more diffuse band, making it hard to assess the glycosylation status of this particular construct.

To facilitate the discrimination between singly and multiply glycosylated molecules, Stt3p constructs with a Suc2 insertion at various positions were also truncated after amino acid residue 536. The site of truncation was chosen about 90 residues downstream of the last predicted TM segment to avoid any possible misinsertion of transmembrane segments into the membrane when truncated between potential TM domains. Moreover, to probe the correct translocation of the C terminus of the protein to the ER lumen, a new *N*-glycan site was generated at the end of the truncated Stt3p. Membrane fractions were prepared from yeast transformants carrying these constructs and treated with Endo H (Fig. 2C). The difference between one glycosylation (due to the lack of three glycosylations of Suc2 reporter if located in cytosol but one from the C terminus) and four glycosylation (three glycosylations from Suc2 domain if oriented to the luminal side of the membrane and one from the C terminus) in a truncated Stt3p was unambiguously resolved in 10% SDS-PAGE (Fig. 2C). The mobility shift upon Endo H treatment clearly showed that the Suc2 reporters inserted after amino acid residues 105, 113, and 354 in the truncated Stt3p were glycosylated, whereas the reporters inserted after amino acid residue 139, 385, and 440 were

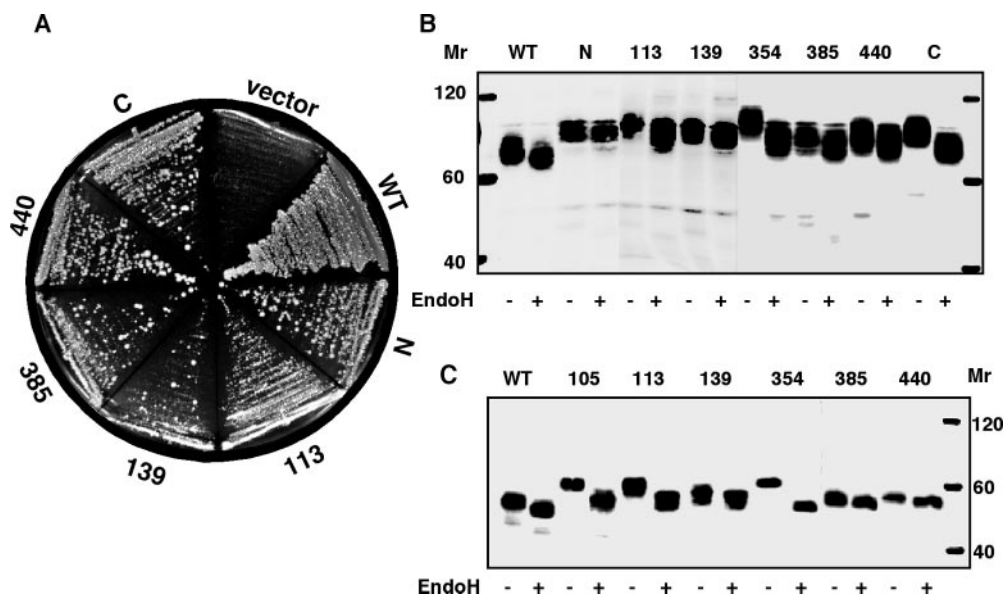


**FIG. 2. Functional complementation of the yeast *stt3* deletion by *Stt3p* constructs with *Suc2* insertions.** The positions of the *Suc2* insertion are indicated. *A*, the growth of constructs transformed into the *stt3* deletion strain and selected for *Suc2* insertion constructs complementing the loss of wild-type (*WT*) *STT3* on 5FOA plates. *B*, the glycosylation status of the full-length *Stt3p* with a *Suc2* insertion assayed by Endo H digestion. *C*, the glycosylation status of the truncated *Stt3p* with a *Suc2* insertion assayed by Endo H digestion. In *B* and *C*, gels were probed by Western blotting with a hemagglutinin antibody.

not (Fig. 2C). Taken together with the results obtained for the full-length *Stt3p*/*Suc2* constructs, we conclude that the loops corresponding to amino acid residues 139, 385, and 440 are on the cytosolic side, whereas those corresponding to amino acid residues 105, 113, and 354 are on the luminal side of the ER membrane.

We finally prepared constructs in which *Stt3p* was truncated near the C-terminal end of predicted loops and fused to the *Suc2*/*His4C* dual reporter domain. A major advantage of using this dual reporter is that a cytosolic orientation of the fusion domain can be confirmed by growth on a selective medium (in addition to the absence of *N*-glycosylation) and *vice versa* for a luminal orientation. The C-terminal fusions at residues 78, 140, 199, 340, and 386 were all sensitive to Endo H digestion and failed to grow on media supplemented with histidinol (Fig. 3), confirming that these regions reside in the lumen of the ER. For unknown reasons, two bands were observed for the fusion at residue 140, both of which were Endo H-sensitive.

The fusions at residues 235 and 437 were insensitive to Endo H, and the one at residue 296 was partially sensitive. Cells carrying all three constructs grew on the selective media supplemented with histidinol. For the fusions at residues 235 and 437, the results clearly suggest a cytosolic location of the reporter domain, whereas for the fusion at residue 296, a cytosolic location of the reporter domain seems likely even if not absolutely certain.

In two cases, the invertase fragment insertion and the C-terminal reporter fusion approaches gave conflicting results. The *Suc2* insertion at residue 139 in full-length *Stt3p* was not glycosylated, whereas the C-terminal reporter fusion at residue 140 was glycosylated and did not support growth on histidinol. Likewise, the *Suc2* insertion at residue 385 was not glycosylated, whereas the C-terminal reporter fusion at residue 386 was glycosylated and did not grow on histidinol. These cases are discussed further below.

**Mouse *STT3-A***—To investigate the topology of mouse *STT3-A*, we used glycosylation mapping (23–25) to determine the location of the *N*- and *C*-terminal ends of the protein and of the predicted loops. When expressed *in vitro* in the presence of microsomes, wild-type *STT3-A* was inserted into the microso-

mal membrane with the C-terminal domain in the lumen, as seen by the glycosylation of one or more of the three acceptor sites for *N*-linked glycosylation (Asn<sup>537</sup>-Arg-Thr, Asn<sup>544</sup>-Asn-Thr, Asn<sup>548</sup>-Asn-Thr) present in this domain (Fig. 4A). As detailed below, no glycosylation was observed for the fourth potential acceptor site in *STT3-A*, Asn<sup>381</sup>-Leu-Ser. This site is situated at the end of a predicted transmembrane segment between residues 361 and 383 and is presumably not glycosylated since *N*-linked glycosylation in the microsomes system requires a minimum distance of 10–15 residues between the glycosylation site and the nearest transmembrane segment (26–28).

When translated both in the absence and in the presence of microsomes, all constructs gave rise to a full-length (Fig. 4A, *FL*) protein but also to a prominent, shorter fragment (Fig. 4A, *F*), which migrated during SDS-PAGE electrophoresis at about half the molecular weight of the full-length protein (Fig. 4A). To check whether this shorter product could also be used for topology mapping, we first determined whether it originates from the *N*- or *C*-terminal part of *STT3-A*. We thus translated a series of C-terminally truncated version (198, 280, 310, 498, 543 residues long) of *STT3-A* in the absence of microsomes (Fig. 4B). As the fragment was not seen for the three shortest constructs but was present in the longer ones, it clearly represents the *N*-terminal ~340 residues of *STT3-A*. Whether it results from proteolysis or premature termination of the full-length protein is unclear, but since it is produced in the absence of microsomes and thus cannot result from an ER-bound proteolytic activity, we favor the latter possibility. The fragment is not glycosylated when *STT3-A* is translated in the presence of microsomes (Fig. 4A (lanes 2 and 3)), again as expected for an *N*-terminal fragment, since the first potential glycosylation site in *STT3-A* is at Asn<sup>381</sup>.

For the topology study, an acceptor site (Asn-Ser-Thr) for *N*-linked glycosylation was inserted into predicted loops at residues 2, 56, 74, 78, 185, 340, 385, 441, and 515 (constructs N2, N56, etc.) (Fig. 4A and Table I). Since the mobility shift resulting from the addition of one extra glycan to the full-length protein is somewhat difficult to resolve in the gel, we used both the *F*-fragment and, for some of the constructs, the

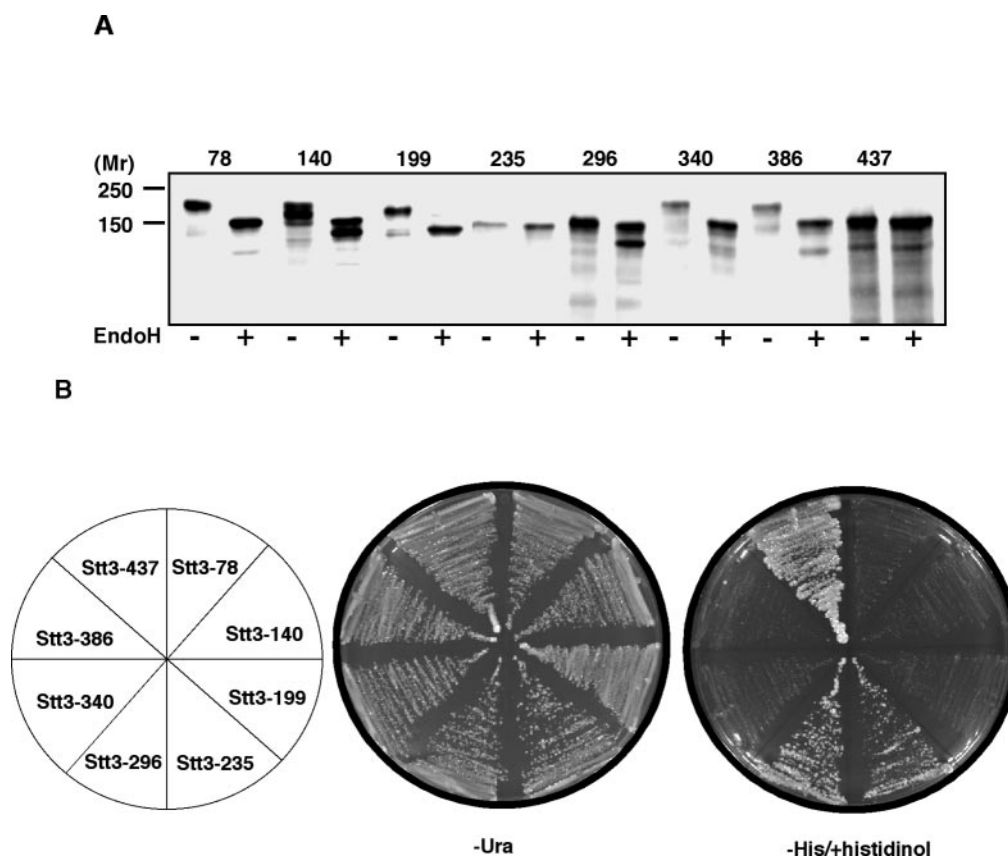


FIG. 3. Investigation of yeast Stt3p topology by C-terminal Suc2/His4C fusions. *A*, the glycosylation status of the Suc2/His4C fusions assayed by Endo H digestion and Western blotting with a hemagglutinin antibody. *B*, the growth of the Suc2/His4C fusions on  $-His$  plates supplemented with histidinol.

versions truncated at residue 538 in the luminal C-terminal domain (and thus lacking the three endogenous glycosylation sites in this domain) (Fig. 4C) to assess the glycosylation status of the engineered sites. To verify that the observed mobility shifts in both the full-length protein and the F-fragment are caused by *N*-linked glycosylation, Endo H digestion was carried out on wild-type STT3-A and construct N56 (Fig. 4D).

The F-fragment was found to be glycosylated in constructs N56, N74, N78, and N340 but not in wild-type STT3-A or in constructs N2, N385, and N515 (Fig. 4A). These results were confirmed using C-terminally truncated constructs for wild type, N340, and N515 (Fig. 4C). Note that the N340 site is rather inefficiently glycosylated in the  $\sim 340$ -residue-long F-fragment (but efficiently glycosylated in the longer F1 product), consistent with earlier observations that glycosylation sites located close to the C terminus of a protein are only inefficiently modified (29). The lack of glycosylation of the F1-fragment of wild-type STT3-A also shows that the endogenous Asn<sup>381</sup> site mentioned above is not glycosylated in STT3-A.

The predicted loop around residue 441 was also targeted. This loop is in itself too short to be glycosylated even if located in the ER lumen (28). For this reason it was extended to a total length of 43 residues, with the engineered glycosylation site placed in the middle. No glycosylation was seen in the context of the truncated construct (F1-fragment) (Fig. 4C). Since the engineered glycosylation site is placed well beyond the C-terminal end of the F-fragment, this should not be modified, as is indeed the case (Fig. 4, A and C).

#### DISCUSSION

This study reports a detailed topology mapping of STT3, the catalytic subunit of OT, from two different organisms, yeast and mouse. STT3 is highly conserved throughout its length (see

Supplementary Material S1), and the yeast and mouse proteins exhibit striking similarities in hydrophobicity profiles. Thus, it seems reasonable to assume that the membrane topology of the yeast and mouse STT3 homologues will be the same. Despite the sequence similarity, the topology predicted by TMHMM is different for the two proteins (Fig. 1). The topology predicted for the yeast protein has the large C-terminal domain located in the ER lumen, in agreement with previously published experimental data (2). We have used a combination of glycosylation site engineering and reporter fusion techniques both in *S. cerevisiae* and in a mammalian *in vitro* transcription/translation system to determine the topology of the two STT3 proteins; the results are summarized in Table I.

Glycosylation sites placed before the first predicted TM of both the yeast and the mouse proteins are not modified, pointing to a cytosolic location of the N terminus. Three engineered glycosylation sites in the first predicted luminal loop (constructs N56, N74, N78) are efficiently modified, and the Suc2/His4C reporter fusions at residues 78, 105, and 113 in the same loop also have a luminal location. The TMHMM predicts the first TM of Stt3p as a possible cleavable signal sequence; however, the results showing that a Suc2 insertion at the N terminus of yeast Stt3p rescued the loss of wild type (Fig. 2A) and that the fusion protein migrated more slowly than the wild type during SDS-PAGE (Fig. 2B) indicate that it is not cleaved. Although TMHMM predicts a TM between residues 79 and 101 of yeast Stt3p and residues 81 and 103 of mouse STT3-A with the following loop in the cytosol, the results for both the invertase insertions after residues 105 and 113 of yeast Stt3p and the engineered glycosylation sites (constructs N74 and N78) of mouse STT3-A indicate that this loop remains in the lumen (a TM in this location would bring the glycosylation site in con-

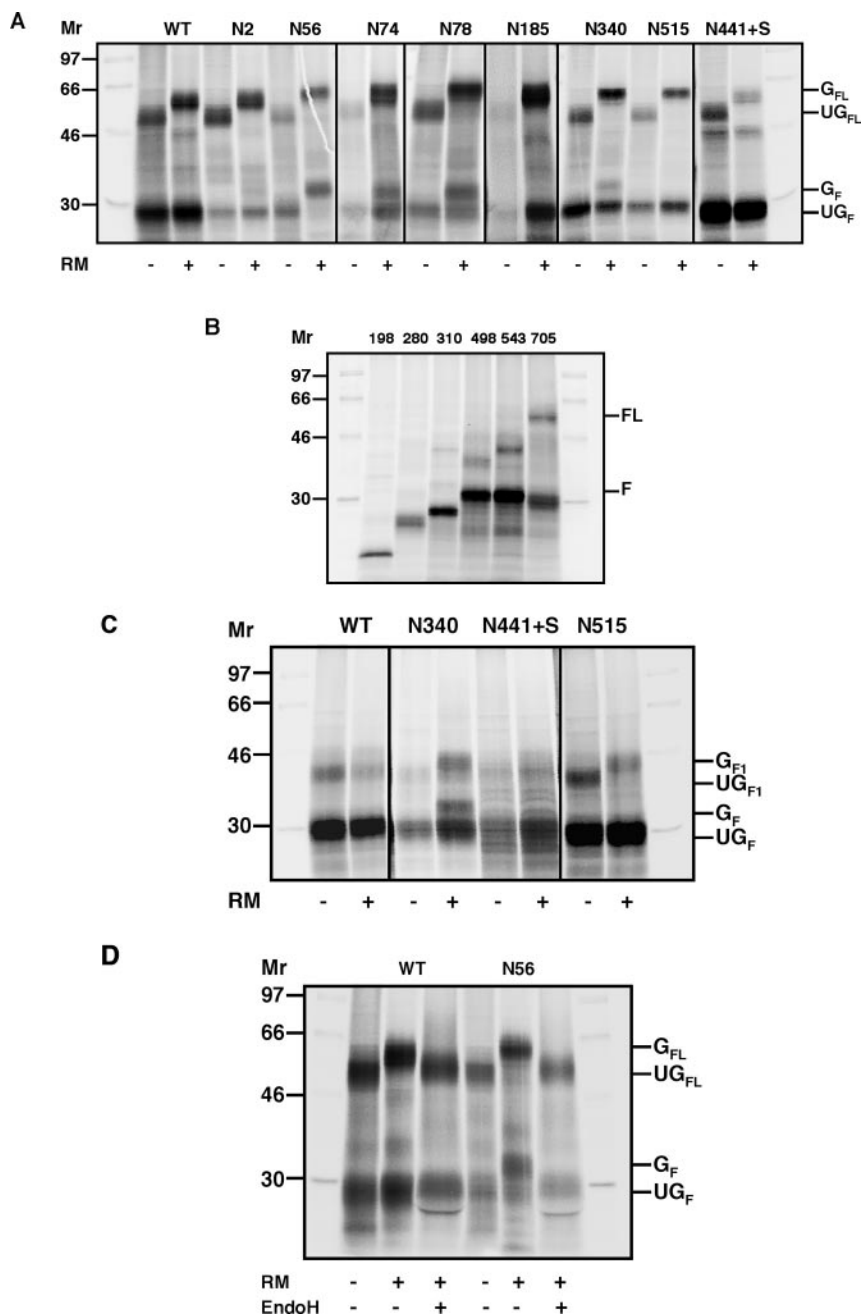


**FIG. 4. Investigation of mouse STT3-A topology by *in vitro* translation.** The position of the Asn residue in the engineered NST glycosylation acceptor sites is indicated above each lane. *S* indicates the insertion of a 10-residue-long spacer sequence at residue 441. **A**, *in vitro* translation in the absence (–) or presence (+) of rough microsomes (*RM*) of full-length protein containing both the three endogenous acceptor sites at Asn<sup>537</sup>, Asn<sup>544</sup>, and Asn<sup>548</sup> and an engineered site in different position (constructs N2, N56, N74, N78, N185, N340, N515, and N441). WT, wild type; *G*, glycosylated product; *UG*, unglycosylated product; *FL*, full-length product, *F*, N-terminal fragment corresponding approximately to residues 1–340. **B**, *in vitro* translation in the absence of microsomes of N-terminal fragments with lengths ranging from 189 residues to the full-length protein (705 residues). **C**, *in vitro* translation in the absence (–) or presence (+) of rough microsomes of constructs WT, N340, N441, and N515 truncated at amino acid residue 538. *FL*, product corresponding to residues 1–538. **D**, *in vitro* translation in the absence (–) or presence (+) of rough microsomes of constructs WT and N56 followed by Endo H digestion.

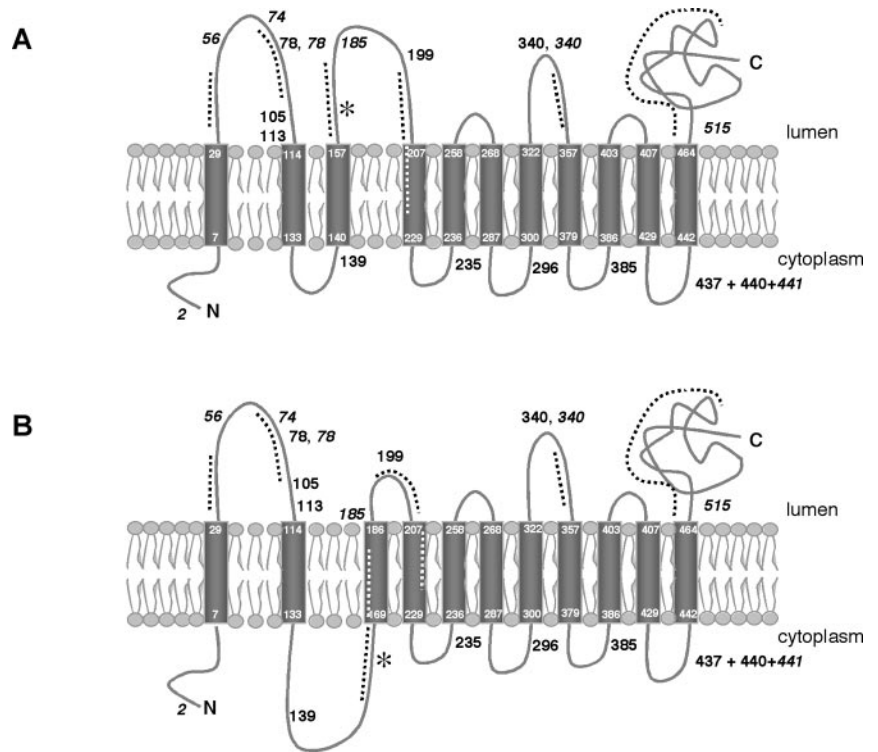
struct N78 too close to the membrane for glycosylation to occur (26–28)).

The invertase insertion after residue 139 is not glycosylated, indicating a cytosolic orientation of this loop, but a reporter fusion to the neighboring residue 140 is glycosylated and does not support growth on histidinol, suggesting a luminal orientation. The location of the corresponding loop thus cannot be deduced with certainty. The location of the loop region around residue 385 must likewise be regarded as uncertain, as again the results for the insertion after residue 385 and the reporter fusion at residue 386 do not agree. Nevertheless, since the invertase insertions after residues 113 and 385 do not inactivate the function of Stt3p (Fig. 2A), they more likely represent the correct membrane topology as compared with the truncation data in which a functional assay cannot be carried out. The results for all the remaining engineered glycosylation sites, invertase insertions, and Suc2/His4C reporter fusion in both the yeast and the mouse proteins agree with the TMHMM prediction for yeast Stt3p.

Using all the experimental data (but excluding the results for the truncations at residues 140 and 386 of yeast Stt3p and the N185 construct for mouse STT3-A; see below) as constraints on the TMHMM predictor (30), we obtained the 11 TM model shown in Fig. 5A. It is of interest that this model places all the highly conserved sequence elements in the lumen of the ER, where the enzymatic catalysis occurs.

A recent genetic study by Chavan *et al.* (31) has reported that the N-terminal domain of Stt3p is important for interactions with the protein kinase C cascade in yeast and that the conserved segment 158–168 (Fig. 5, *star*) may interact with some cytosolic component in the Pkc1p cascade. In the model shown in Fig. 5A, this segment is located in the ER lumen. If, however, a cytosolic location of residues 158–168 is included as an additional constraint, TMHMM predicts the topology shown in Fig. 5B, with TM3 shifting from residues 140 to 157 to residues 169 to 186. In an attempt to differentiate between these two models, we engineered a glycosylation acceptor site into positions 185–187 (construct N185). As seen in Fig. 4A, the F-

**FIG. 5. Topology models for STT3.** Experimentally determined points are indicated in *black letters (Roman text for yeast and italics for mouse)*. The predicted residues of TMs are indicated in *white letters*. *Dashed lines* indicate segments that are highly conserved between the yeast and mouse proteins (amino acids 32–53, 68–90, 154–172, 199–221, 342–353, and 494–593). The *star* indicates the location of residues 158–168, proposed to interact with a component of the Pkc1p cascade (31). The model in *panel A* is the TMHMM prediction constrained by the experimental results derived in this work; the model in *panel B* has the additional constraint that residues 158–168 are cytosolic.



fragment in this construct is not glycosylated. This is the expected result for the model in Fig. 5B in which N185 is too close to TM3 to be glycosylated (26–28), whereas if the model in Fig. 5A is correct, construct N185 should be glycosylated. On balance, we thus favor the model presented in Fig. 5B.

In summary, we have derived a common model for the membrane topology of STT3 from yeast and mouse. It has 11 TMs, the N terminus in cytosol and the C terminus in lumen, and most of the highly conserved segments on the luminal side of the ER membrane.

**Acknowledgments**—We gratefully thank Prof. William Lennarz for providing yeast strains and plasmids, Prof. Arthur E. Johnson for providing rough microsomes, Prof. Joseph Merregaert for providing a mouse STT3 plasmid (Itm1 cDNA), and Karin Melén for TMHMM predictions.

#### REFERENCES

- Yoshida, S., Ikeda, E., Uno, I., and Mitsuzawa, H. (1992) *Mol. Gen. Genet.* **231**, 337–344
- Zufferey, R., Knauer, R., Burda, P., Stagljar, I., te Heesen, S., Lehle, L., and Aebi, M. (1995) *EMBO J.* **14**, 4949–4960
- Yan, Q., and Lennarz, W. J. (2002) *J. Biol. Chem.* **277**, 47692–47700
- Kelleher, D. J., Karaoglu, D., Mandon, E. C., and Gilmore, R. (2003) *Mol. Cell Biol.* **23**, 101–111
- Nilsson, I., Kelleher, D. J., Miao, Y., Shao, Y., Kreibich, G., Gilmore, R., von Heijne, G., and Johnson, A. E. (2003) *J. Cell Biol.* **161**, 715–725
- Wacker, M., Linton, D., Hitchen, P. G., Nita-Lazar, M., Haslam, S. M., North, S. J., Panico, M., Morris, H. R., Dell, A., Wren, B. W., and Aebi, M. (2002) *Science* **298**, 1790–1793
- Burda, P., and Aebi, M. (1999) *Biochim. Biophys. Acta* **1426**, 239–257
- Kim, H., Yan, Q., Von Heijne, G., Caputo, G. A., and Lennarz, W. J. (2003) *Proc. Natl. Acad. Sci. U. S. A.* **100**, 7460–7464
- Strahl-Bolsinger, S., and Scheinost, A. (1999) *J. Biol. Chem.* **274**, 9068–9075
- Kim, H., Melen, K., and von Heijne, G. (2003) *J. Biol. Chem.* **278**, 10208–10213
- Wilhovský, S., Gardner, R., and Hampton, R. (2000) *Mol. Biol. Cell* **11**, 1697–1708
- Johansson, M., Nilsson, I., and von Heijne, G. (1993) *Mol. Gen. Genet.* **239**, 251–256
- Hong, G., Deleersnijder, W., Kozak, C. A., Van Marck, E., Tylzanowski, P., and Merregaert, J. (1996) *Genomics* **31**, 295–300
- Kozak, M. (1989) *Mol. Cell Biol.* **9**, 5073–5080
- Mingarro, I., Nilsson, I., Whitley, P., and von Heijne, G. (2000) *BMC Cell Biol.* **1**, 3 <http://www.biomedcentral.com/1471-2121/1/3>
- Nilsson, I., Whitley, P., and von Heijne, G. (1994) *J. Cell Biol.* **126**, 1127–1132
- Liljeström, P., and Garoff, H. (1991) *J. Virol.* **65**, 147–154
- Krogh, A., Larsson, B., von Heijne, G., and Sonnhammer, E. L. (2001) *J. Mol. Biol.* **305**, 567–580
- Deak, P. M., and Wolf, D. H. (2001) *J. Biol. Chem.* **276**, 10663–10669
- Gilstring, C. F., and Ljungdahl, P. O. (2000) *J. Biol. Chem.* **275**, 31488–31495
- Karaoglu, D., Kelleher, D. J., and Gilmore, R. (1997) *J. Biol. Chem.* **272**, 32513–32520
- Li, G., Yan, Q., Nita-Lazar, A., Haltiwanger, R. S., and Lennarz, W. J. (2005) *J. Biol. Chem.* **280**, 1864–1871
- Devoto, A., Piffanelli, P., Nilsson, I., Wallin, E., Panstruga, R., von Heijne, G., and Schulze-Lefert, P. (1999) *J. Biol. Chem.* **274**, 34993–35004
- van Geest, M., Nilsson, I., von Heijne, G., and Lolkema, J. S. (1999) *J. Biol. Chem.* **274**, 2816–2823
- von Heijne, G. (1998) *Acta Physiol. Scand.* **163**, 17–19
- Nilsson, I., and von Heijne, G. (1993) *J. Biol. Chem.* **268**, 5798–5801
- Whitley, P., Nilsson, I. M., and von Heijne, G. (1996) *J. Biol. Chem.* **271**, 6241–6244
- Popov, M., Tam, L. Y., Li, J., and Reithmeier, R. A. (1997) *J. Biol. Chem.* **272**, 18325–18332
- Nilsson, I., and von Heijne, G. (2000) *J. Biol. Chem.* **275**, 17338–17343
- Melen, K., Krogh, A., and von Heijne, G. (2003) *J. Mol. Biol.* **327**, 735–744
- Chavan, M., Rekowicz, M., and Lennarz, W. (2003) *J. Biol. Chem.* **278**, 51441–51447